

Raman spectroscopy of BN-SWNTs

R. Arenal de la Concha^{1,2}, L. Wirtz², J.Y. Mevellec³, S. Lefrant³, A. Rubio²,
A. Loiseau¹

¹ LEM, Onera-Cnrs, 29 Avenue de la Division Leclerc, BP 72, 92322 Châtillon, France

² Dpto. Física de Materiales, Facultad de Químicas, UPV-DIPC,
Apdo. 1072, 20018 San Sebastian, Spain

³ Laboratoire de Physique Cristalline, IMN, BP 32229, 44322 Nantes, France

Abstract. We present here the results on the vibrational properties on the BN-SWNTs coupled with a study of the synthesis material by transmission electron microscopy. Phonon modes have been investigated by Raman spectroscopy with laser excitation wavelengths in the range from 363.8 to 676.44 nm. The assignment of the modes is developed using density-functional calculations.

INTRODUCTION

Raman spectroscopy has been proved to be an efficient and nondestructive technique for characterizing C-NTs, since it provides useful information not only on the geometric, electron and phonon structure, but also on physical effects [1,2]. In the case of boron nitride NTs (BN-NTs), the experimental progress on studying their physical properties has been slowed because the quantity of single wall (SW) NTs was very limited. Recently, a continuous laser vaporization process [3] was reported that produced BN-SWNTs in gram quantities.

In this paper, we present results the first experimental study of Raman scattering on SW-BNNTs and *ab initio* calculations in support of experimental data.

EXPERIMENT

Details of the laser-assisted process used to synthesize our BN-NTs have appeared elsewhere [3]. Briefly, an h-BN target was ablated with continuous CO₂ laser under a nitrogen flow at a pressure 1 bar.

Transmission electron microscopy (TEM) was carried out using a Jeol 4000FX (at 400kV) and the chemical compositions were examined using energy electron spectroscopy (EELS) in a VG501 (at 100kV). Raman spectra were collected with the Jobin-Yvon T64000 Raman spectrometer using in the visible range a microscope in a backscattering geometry. The laser excitation wavelengths of 363.8, 457.9, 488, 514.5 and 676.44 nm were used. Laser beam was focused into a spot size about few μm in diameter on the sample providing to explore different areas and its power was below 10 mW for preventing sample burning.

RESULTS AND DISCUSSION

Description of the samples

A TEM image in Fig. 1 a) exhibits a general view of the synthesis products. The two dominant structures are nanotubes and closed polyhedral structures. From TEM analysis, we

estimated that the yield of BN-NTs could be of the order of 25% of the ablated material and that about 80% of the NTs are single walled, and 15% double walled nanotubes.

The BN-SWNTs appear either as individual tubes or as bundles. Fig. 1 b) is a typical HRTEM image, showing a bundle and a SWNT. The diameter distribution is centered at 1.4 nm (FWHM=0.6 nm) and 1.6 nm (FWHM=0.3 nm) for isolated tubes and bundles, respectively. The tube length is between 100 and 400 nm with a few tubes exceeding 1000 nm.

The bonding state and chemical composition of the individual nanostructures were determined by EELS. The spectra taken from the NTs show clearly the presence of boron and nitrogen in the sp^2 type of bonding, and confirmed the expected BN stoichiometry [4].

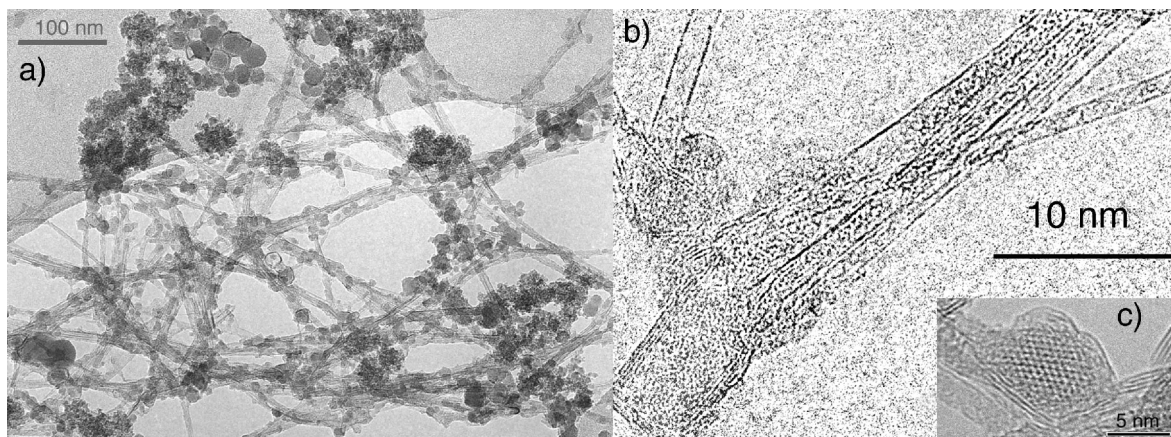


FIGURE 1 a) Low magnification TEM image of a BN sample, showing bundles of SW-BNNTs, cages of h-BN and clusters of nanoparticles b) HRTEM picture of a bundle of SW-BNNTs and two isolated SW-BNNTs c) The inset shows a HRTEM image of a boron nanocrystal.

Polyhedral nanostructures consists of particles either nested into h-BN shells or located at the tip of NTs. The particles are identified from EELS analysis as having a pure boron core. This core was often crystalline and corresponds to a rhombohedral form (Fig. 1 c)). Very often its surface is covered by a thin boron oxide layer [4].

Raman Experiments

The Raman experiments carried out on BN-NTs samples revealed to be very delicate for several reasons. First, the samples appeared rather heterogeneous at the scale of the laser beam size. Depending on the spot position, different spectra were recorded either resembling that of pure h-BN [5] or assigned to NTs rich areas. Second, some regions of the samples were easily burnt even with lower laser power used. Finally a strong luminescence is always observed whatever the spot position, the temperature and the wavelength.

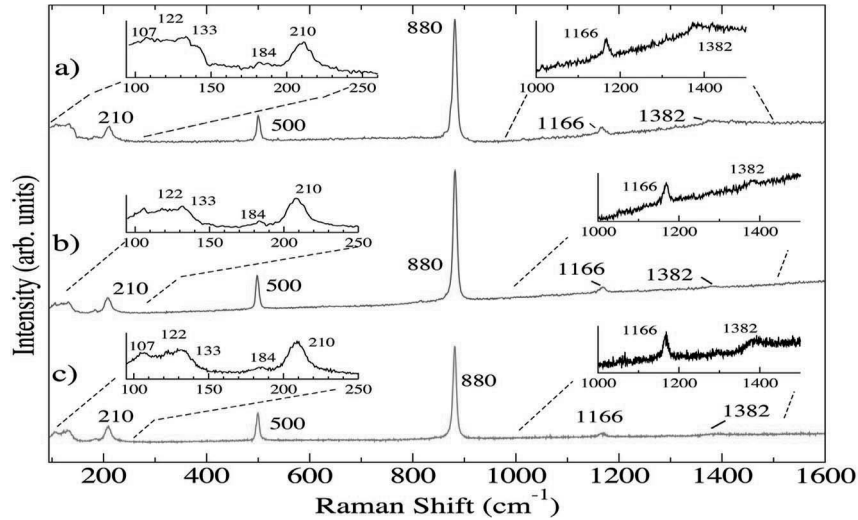


FIGURE 2 Room temperature Raman spectra of unpurified SW-BNNTs at the same area and at different laser energies (a) 457.9; b) 488; c) 514.5 nm). In inset we can see the low and high frequency regions.

Fig. 2 shows the Raman spectra associated to BN-NTs for different wavelengths at room temperature. No dependence on the excitation wavelength is observed. In contrast to C-NTs [2], the absence of resonant modes even at 363.8 nm confirms the insulating character of BN NTs and indicates a gap larger than 3.4 eV. Many peaks can be distinguished in three different regions of the spectra. The low-frequency region displays a set of peaks at 107, 122, 133, 184 and 210 cm^{-1} [5]. In the high-frequency range, two peaks at 1166 and 1382 cm^{-1} can be discerned. Finally, sharp and intense peaks at 500 and 880 cm^{-1} are seen in the medium range.

Calculations and modes assignment

We have performed an *ab initio* density-functional study under local density approximation, using the code ABINIT [6]. We have employed Troullier-Martins pseudopotentials and a plane-wave energy cut-off of 80 Ry. A more detailed analysis is presented in [7]. Results are presented in Fig.3 for a selection of tubes together with the variation of the phonon frequencies obtained by the zone-folding (ZF) method as a function of the tube diameter. Except for the breathing mode which cannot be calculated with the ZF method, Fig. 3 attests for an excellent agreement between *ab initio* values and frequencies derived from ZF.

We now turn to the comparison between experiments and theory. In the low frequencies range, we can identify the radial breathing modes (RBM). Owing to the diameter distribution of our samples, the calculated RBM and others active low frequency modes are consistent with the peaks observed at 107, 122, 133 and 184 cm^{-1} . The peak at 210 cm^{-1} can be associated with a tangential mode (E_1).

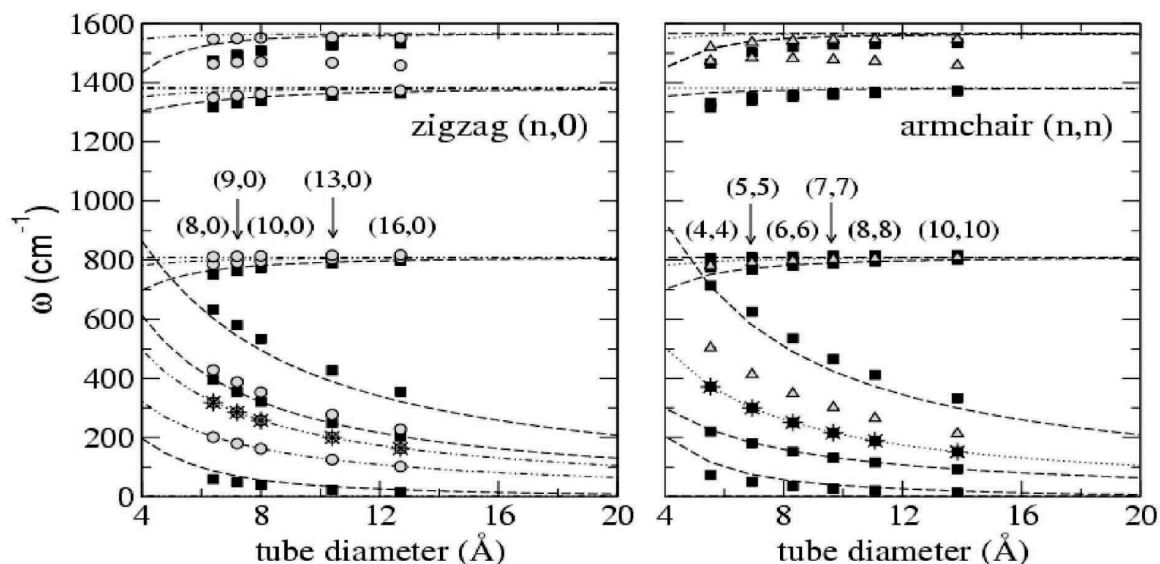


FIGURE 3 Phonon frequencies of Raman and IR active modes for (infinitely long) zigzag and armchair NTs as a function diameter. Comparison of *ab initio* values (symbols) with ZF method (lines). Squares/dashed lines: only Raman active; triangles/dotted lines: only IR active; circles/dash-dotted lines: Raman and IR active. The RBM is in addition marked by asterisk. For zigzag-tubes the IR modes are a subset of the Raman ones, while for armchair tubes, the two sets are disjoint.

The broad and weak band at 1382 cm^{-1} can be easily associated with a signal of tubes (A_g and E_{1g} modes). The weakness intensity of the peaks is partially due a strong luminescence background.

The assignment the most intense peaks at 500 and 880 cm^{-1} is not possible with the frequencies obtained from the calculations. Furthermore, these peaks cannot be attributed to the contaminants detected by TEM and EELS in the samples (amorphous C, Ca, amorphous BN, SiO_2 and B_2O_3). In particular, we do not observe features typical of Boron (frequencies and wavelength dependence [5] even though boron particles are mixed with the tubes. We therefore suspect that the peaks are due to another contaminant which has not yet been identified but which is only present in the areas containing the nanotubes.

CONCLUSION

We have presented a combined study of first-principle calculations for phonon modes and Raman experiments on BN-SWNTs synthesized by laser vaporization h-BN. The non resonance of Raman spectra at excitation wavelengths ranging from 676.44 to 363.8 nm indicates a band gap larger than 3.4 eV . Peaks at low and high frequencies have been identified as a clear signal of the tubes in spite of their weakness. Thin peaks at medium frequencies are not yet explained and are expected to arise from an unknown contaminant.

ACKNOWLEDGMENTS

This work has supported by a TMR contract COMELCAN (HPRN-CT-2000-00128).

REFERENCES

- 1 R. Saito, G. Dresselhaus, M. S. Dresselhaus, *Physical properties of C-NTs*, Imperial College Press, London, 1998; M. S. Dresselhaus, G. Dresselhaus, Ph. Avorius (Eds.), *C-NTs: synthesis, structure, properties and applications*, Springer-Verlag, Berlin, 2001.
- 2 A. M. Rao, E. Richter, S. Bandow, B. Chase, P. C. Eklund, K. A. Williams, S. Fang, K. R. Subbaswamy, M. Menon, A. Thess, R. E. Smalley, G. Dresselhaus, M. S. Dresselhaus, *Science* **275**, 187 (1997).
- 3 R. S. Lee, J. Gavillet, M. Lamy de la Chapelle, A. Loiseau, J.-L. Cochon, D. Pigache, J. Thibault, F. Willaime, *Phys. Rev. B* **64**, 121405 (2001).
- 4 R. Arenal de la Concha, A. Vlandas, O. Stephan, A. Loiseau, (to be published).
- 5 R. Arenal de la Concha, L. Wirtz, J.Y. Mevellec, S. Lefrant, A. Rubio, A. Loiseau, submitted *Chem. Phys. Lett.* (2003).
- 6 The ABINIT code is a common project of the Université Catholique de Louvain, Corning Incorporated, and other contributors (URL <http://www.abinit.org>)
- 7 L. Wirtz, R. Arenal de la Concha, A. Loiseau, A. Rubio, submitted *Phys. Rev. B* (2003).